International Journal of Civil and Structural Engineering– IJCSE
Volume 1 : Issue 4 *[ISSN 2372-3971]*
Publication Date : 27 December,2014

Moving load on a railway track – finite difference solution

N Prasad, S Chandra

***Abstract*—This study investigates the response of a railway track modelled as an Euler-Bernoulli beam placed on a two parameter foundation with the inclusion of an additional elastic layer representing the subgrade. Uplift, settlement and bending moment caused by variations in velocity, damping and stiffness of subgrade have been found numerically. Changes in the subgrade stiffness are found to have relatively insignificant effect on the behavior of the beam.**

Keywords*—railway track, two parameter model, finite difference method, infinite beam, elastic foundation, moving load *(key words)

I. Introduction

Mallik et al. (2006) found the analytical solution of the problem of a moving load on an elastic foundation represented by Pasternak model (Pasternak, 1954). This study builds on that work by considering changes in the behaviour of an infinite Euler-Bernoulli beam resting on a two parameter foundation model with respect to different subgrade stiffness values. The model has been modified to include an additional elastic layer representing the subgrade. A numerical method has been employed to determine the deflection and bending moment profiles of the beam.

II. Two Parameter Model

Fig. 1 illustrates the two parameter model used in this study. It contains a shear layer and two elastic layers representing the ballast and subgrade layers. This model builds on the work of Mallik et al. (2006).

Equation (1), as obtained by Mallik et al. (2006), was numerically solved to find the deflection profile of an Euler-Bernoulli beam in this study.

$$\frac{d^4w}{d\xi^4} - 2c_1\frac{d^2w}{d\xi^2} + b^2w + 2av^2\frac{d^2w}{d\xi^2} - dv\frac{dw}{d\xi} = 0 \qquad (1)$$

Nikeesh Prasad
University of Melbourne
Australia

Sarvesh Chandra
Indian Institute of Technology Kanpur
India

with

$$a = \frac{\rho}{2EI},\ b^2 = \frac{k_{eq}}{EI},\ c_1 = \frac{k}{2EI},\ d = \frac{c}{EI}$$

where w = transverse deflection of the beam (m); E = Young's modulus of the beam material (N/m^2); I = second moment of area of the beam cross-section about its neutral axis (m^4); k_{eq} = equivalent spring constant of the soil (N/m^2); k = shear parameter (second parameter) of the soil (N); ρ = mass per unit length of the beam (kg/m); c = coefficient of viscous damping per unit length of the beam (Ns/m^2); P = applied moving load (N); and ξ = modified space coordinate measured along the length of the beam (m).

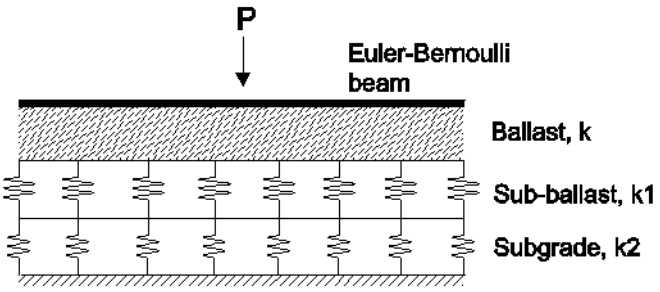

Figure 1. Two parameter model

A. *Modelling the subgrade layer*

In this paper the ballast is modelled by a shear layer and the sub ballast and subgrade layers of the railway track are modelled by two layers of Winkler springs. The spring constant of the sub-ballast and subgrade layers can be incorporated into (1) by using an equivalent spring constant k_{eq}, given by the following relationship.

$$\frac{1}{k_{eq}} = \frac{1}{k_1} + \frac{1}{k_2} \qquad (2)$$

where k_1 = spring constant of the sub-ballast (N/m^2); and k_2 = spring constant of the subgrade (N/m^2).

An equivalent system to the one above would be a two parameter model with a single elastic layer with spring constant of k_{eq}.

III. Approximation using the method of finite differences

A numerical method, the finite difference method in particular, was used to solve (1). The central finite-divided-difference approximation formulae used for respective derivatives at i^{th} node are as follows:

$$\omega'(\xi) = \frac{\omega(\xi_{i+1}) - \omega(\xi_{i-1})}{2h}$$

$$\omega''(\xi) = \frac{\omega(\xi_{i+1}) - 2\omega(\xi_i) + \omega(\xi_{i-1})}{h^2}$$

$$\omega^{(3)}(\xi) = \frac{\omega(\xi_{i+2}) - 2\omega(\xi_{i+1}) + 2\omega(\xi_{i-1}) - \omega(\xi_{i-2})}{2h^3}$$

$$\omega^{(4)}(\xi) = \frac{\omega(\xi_{i+2}) - 4\omega(\xi_{i+1}) + 6\omega(\xi_i) - 4\omega(\xi_{i-1}) + \omega(\xi_{i-2})}{h^4} \quad (3)$$

where h = distance between adjacent nodes (m); and Error = $O(h^2)$.

The boundary conditions used at both the ends were:

$$\frac{d\omega}{d\xi} = 0, \quad \omega = 0 \quad (4)$$

Assuming the load is applied at the j^{th} node, an additional boundary condition is created at that point. In this study, the load was applied at the centre of the beam.

$$\left.\frac{d^3w}{d\xi^3}\right|_j = \frac{-P}{2EI} \quad (5)$$

Using the finite divided difference approximation formulae (3) and the boundary conditions, relationships between deflections at the nodes in the vicinity of these boundary conditions were established which were then used to generate the deflection profile of the entire beam. The bending moment diagram was created by differentiating the deflection profile twice using the finite difference method.

A. *Verification of the model*

The numerical model was verified by comparing it to the closed form solution (6) obtained by Mallik et al. (2006). For the undamped case with velocity less than critical, the closed form solution is as follows:

$$\omega_1(\xi) = \frac{Pe^{-\alpha\xi}}{4EI b\alpha\beta}[\alpha \sin\beta\xi + \beta\cos\beta\xi] \qquad \text{for } \xi > 0$$

$$\omega_2(\xi) = \frac{Pe^{\alpha\xi}}{4EI b\alpha\beta}[\beta\cos\beta\xi - \alpha\sin\beta\xi] \qquad \text{for } \xi < 0$$

$$\text{with } \alpha = \sqrt{\frac{b - (av^2 - c_1)}{2}}, \ \beta = \sqrt{\frac{b + (av^2 - c_1)}{2}} \quad (6)$$

The closed-form solution above was used to generate normalised deflection and bending moment profiles (not shown here) using the same normalisation method. Critical values were compared to the numerical model used in this analysis. The numerical model, in this comparison, does not have a subgrade layer present.

The difference in the maximum positive and negative bending moment between the two models was 0.26% and 1.74% respectively. In both cases, the numerical results gave slightly lower values than the closed-form solution.

The deflection profiles indicated that the difference in maximum uplift and settlement between the two approaches were 2.18% and 0.003% respectively. The numerical model produced a higher value for uplift and a marginally smaller value for settlement.

For the purpose of the numerical analysis conducted here, a variance of less than 3% was deemed adequate. Hence, the modelling parameters adopted for the finite difference model were as follows:

- The finite-divided difference approximation formulae had an error of the second order: $O(h^2)$.
- The model contains 25 nodes per metre (non-normalised) of the beam length in the ξ direction.
- Total beam length of 80 metres (non-normalised) was used.

IV. Results and Discussion

Table 1. Soil and beam parameters

Parameter	*Assumed value*
ρ (kg/m)	25
EI (m^4)	1.75×10^6
k_{eq} (N/m^2)	50×10^5
k (N)	666875
P (N)	93.36×10^3

The length of the beam has been normalised by multiplying it by the characteristic length, λ.

$$\lambda = \left(\frac{k_{eq}}{4EI}\right)^{1/4} = \sqrt{b/2} \quad (7)$$

The deflection and bending moment values have been normalised by dividing it by their respective maximum values in the static case.

The following sign convention was used in this study:

Shear force Bending moment

The magnitudes of velocity and damping have been expressed as a ratio of their respective critical values. The definition of the critical values of velocity and damping has been borrowed from Mallik et al. (2006) and modified slightly for this analysis.

$$v_{cr} = \sqrt{\frac{b + c_1}{a}} = \left(\frac{\sqrt{4EIk_{eq}} + k}{\rho}\right)^{1/2} \quad (8)$$

$$d_{cr} = 2\sqrt{2}b\sqrt{a} = \frac{2}{EI}\sqrt{k_{eq}\rho} \quad (9)$$

where v_{cr} = critical velocity; and d_{cr} = critical damping.

The stiffness of the subgrade (k_1) was varied as a percentage of the stiffness of the sub-ballast (k_2).

A. *Varying the velocity ratio*

To observe the effect of the velocity of the moving load on the beam, deflection and bending moment profiles were generated for three sub-critical velocity ratios (Vr). A damping ratio of 30% and a subgrade modulus of elasticity of 50% (of sub-ballast modulus of elasticity) were used.

Figure 2 shows deflection for three values of velocity ratios: 0, 0.25 and 0.5. Maximum deflection occurs under the applied load when the load is stationary and moves behind the load slightly as the velocity increases. Also, the maximum deflection increased by 2.7% and 12% as the velocity increased to a quarter and then half of its critical value respectively.

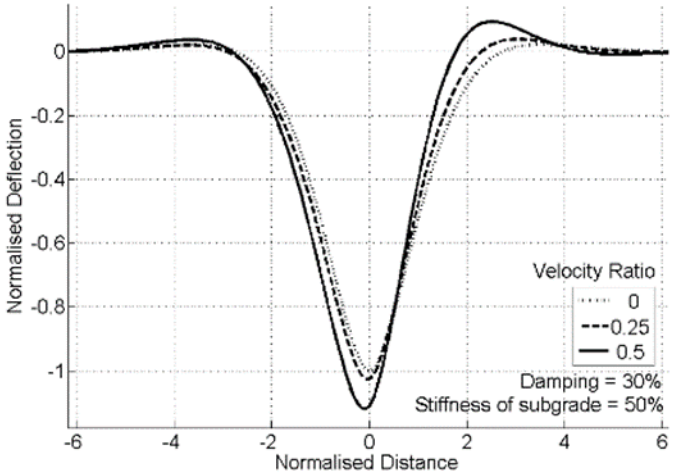

Figure 2. Normalised deflection profile for three subcritical velocity ratios.

No significant uplift is observed behind the load. Ahead of the load however, uplift increases markedly with increase in velocity. At Vr=0.25, uplift is approximately 1.8 times the stationary condition and at Vr=0.5, it is 4.3 times the same.

Figure 3 illustrates the variation in bending moment for the same configuration of loading and velocity ratios as above. The variations in maximum positive bending moment follow the same pattern as the maximum deflection under the load. Sagging moment behind the load is not significant. Ahead of the load, the maximum sagging moment increases 1.2 and 1.7 times the stationary case for velocity ratios of 0.25 and 0.5 respectively.

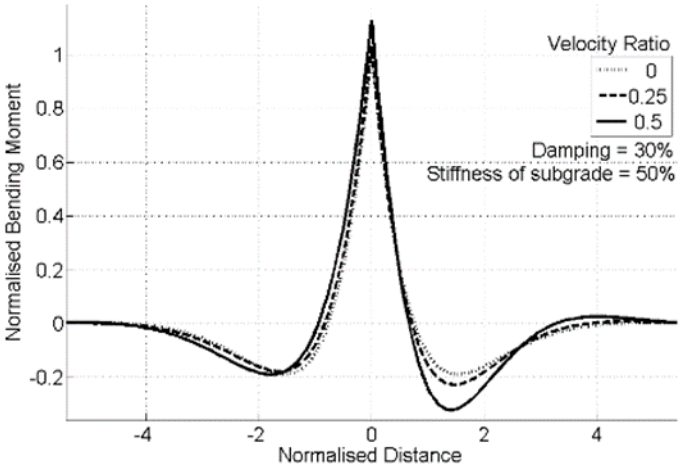

Figure 3. Normalised bending moment profile for three subcritical velocity ratios.

B. *Varying the damping ratio*

Deflection and bending moment profiles were generated for different subcritical damping ratios.

Figure 4 shows a reduction in maximum deflection under the load by 6.3% and 18.8% for 45% and 90% damping ratios respectively. In contrast to variations in velocity ratios, damping variations cause significant changes in uplift behind the load whereas uplift ahead of the load increases only slightly with increases in damping ratio. At damping ratios of 45% and 90%, the maximum uplift is approximately 35% and 2% of that of the undamped case.

Figure 5 shows that maximum positive bending moment follows a similar trend to the maximum deflection observed in Figure 4 with maximum positive bending moment decreasing with increasing damping ratios. The maximum sagging moment both ahead of and behind the applied load however, varies. Behind the applied load, maximum sagging moment is 61.7% and 35.6% of the undamped case for damping ratio of 45% and 90% respectively.

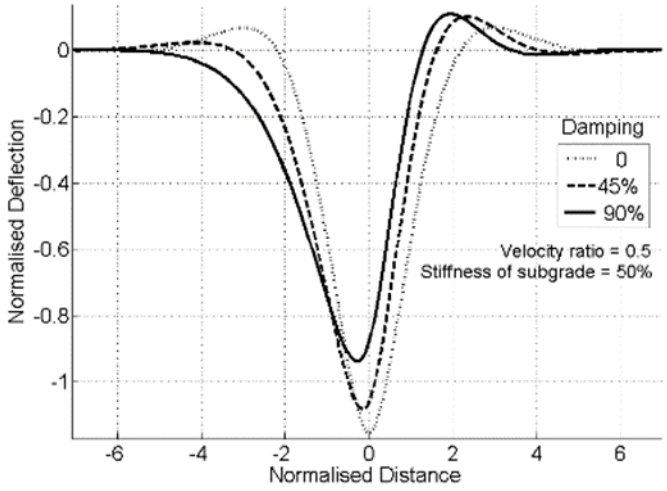

Figure 4. Normalised deflection profile for three subcritical damping ratios.

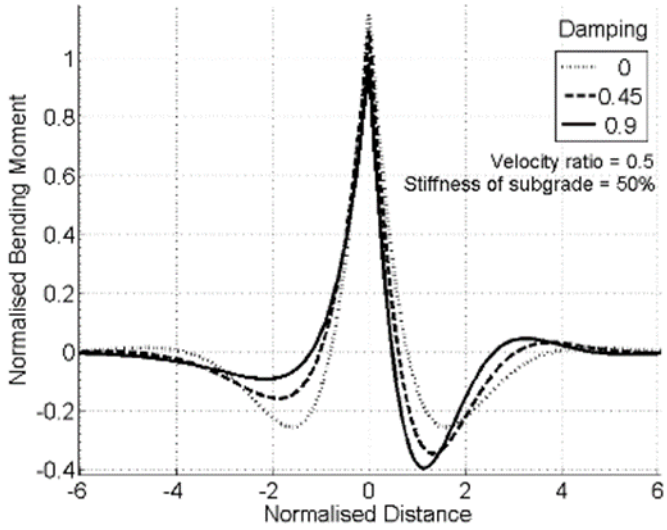

Figure 5. Normalised bending moment profile for three subcritical damping ratios.

C. *Varying the stiffness of the subgrade*

Variation in subgrade stiffness resulted in minor changes in the behaviour of the deflection and bending moment profiles. Comparisons have been made with respect to the case without the subgrade layer. The following tables show the magnitude of maximum deflection or bending moment and its position as a coordinate pair. The first number represents the normalised distance and the second, the respective value of interest.

Table 2. Maximum deflection at different locations on the beam for given subgrade stiffness ratios

Subgrade ratio	*Centre*	*Ahead*	*Behind*
No subgrade	-0.073,-1.118	2.427,0.107	-3.530,0.047
50%	-0.083,-1.120	2.515,0.094	-3.646,0.037
70%	-0.088,-1.120	2.519,0.097	-3.623,0.039
90%	-0.092,-1.199	2.517,0.099	-3.615,0.041

Table 3. Maximum bending moment at different locations on the beam for given subgrade stiffness ratios

Subgrade ratio	*Positive*	*Sagging*	
		Ahead	*Behind*
No subgrade	0,1.1263	1.397,-0.331	-1.839,-0.195
50%	0,1.1277	1.425,-0.320	-1.802,-0.188
70%	0,1.1273	1.414,-0.322	-1.812,-0.190
90%	0,1.1270	1.419,-0.324	-1.785,-0.190

The point of maximum deflection moved between 14% and 24% behind the load as the sub-grade stiffness increased from 50% to 90%. The point of maximum uplift, ahead of and behind the load, moved between 2% and 4%. The magnitude of maximum deflection decreased as the stiffness of subgrade increased however this reduction was miniscule (less than 1%). Additionally, the inclusion of the subgrade with 50% stiffness decreased the uplift ahead of and behind the load by 12% and 21% respectively which then progressively increased as the stiffness was increased.

The maximum positive bending moment increased as the stiffness of the subgrade decreased however, this increase was minute (less than 1%). The maximum sagging moment, ahead of and behind the load, decreased by 3.5% to 4% with a subgrade stiffness of 50% and increased with increasing stiffness.

V. Conclusion

The conclusions of this study are as follows:

1. The behaviour of the beam, with the inclusion of an additional subgrade layer, for varying velocity and damping ratios was relatively consistent with that obtained by Mallik et al. (2006).
2. The point of maximum deflection shifts behind the applied load with increasing stiffness of the subgrade layer.
3. Overall, the effect of varying the subgrade stiffness between 50% and 90% of the stiffness of the sub-ballast is small.

References

[1] Mallik, A. K., Chandra, S. & Singh, A. B. 2006. Steady-state response of an elastically supported infinite beam to a moving load. Journal of Sound and Vibration, 291, 1148-1169

[2] Pasternak, P. L. 1954. Fundamentals of a new method of analyzing structures on an elastic foundation by means of two foundation moduli, Gosudarstvennoe Izdatelstro Liberaturi po Stroitelstvui Arkhitekture (in Russian).